



## Biogenic Silver Nanoparticles (AgNPs) from *Marphysa moribidii* Extract: Optimization of Synthesis Parameters

Nur Syakirah Rabiha Rosman<sup>1,2</sup>, Mohammad Asyraf Adhwa Masimen<sup>1,2</sup>, Noor Aniza Harun<sup>3,4</sup>, Izwandy Idris<sup>5</sup>, Wan Iryani Wan Ismail<sup>1,2\*</sup>

<sup>1</sup>Cell Signaling and Biotechnology Research Group (CeSBTech), Faculty of Science and Marine Environment, Universiti Malaysia Terengganu, 21030 Kuala Nerus, Terengganu, Malaysia

<sup>2</sup>Biological Security and Sustainability Research Group (BIOSES), Faculty of Science and Marine Environment, Universiti Malaysia Terengganu, 21030 Kuala Nerus, Terengganu, Malaysia

<sup>3</sup>Advanced Nano Materials (ANOMA) Research Group, Faculty of Science and Marine Environment, Universiti Malaysia Terengganu, 21030 Kuala Nerus, Terengganu, Malaysia

<sup>4</sup>Higher Institution Centre of Excellence (HiCoE), Institute of Tropical Aquaculture and Fisheries (AKUATROP), Universiti Malaysia Terengganu, 21030 Kuala Nerus, Terengganu, Malaysia

<sup>5</sup>South China Sea Repository and Reference Centre, Institute of Oceanography and Environment (INOS), Universiti Malaysia Terengganu, 21030 Kuala Nerus, Terengganu, Malaysia

**Abstract.** Interest in biogenic silver nanoparticles (AgNPs) is steadily increasing due to the cost-effective, easy, and environmentally friendly way in which they are synthesized. Synthesis using polychaete (*Marphysa moribidii*) extract as a reducing agent is particularly new and has the potential of being applied in various industries. However, biogenic AgNPs require synthesis optimization to increase their stability, yield, and characteristics. To meet these requirements, several synthesis parameters (such as polychaete size (body width), silver nitrate (AgNO<sub>3</sub>) concentration, pH of polychaete crude extract, and the temperature during pre-incubation) and storage conditions were optimized in this study. The optimized conditions for obtaining high yield and stable AgNPs were polychaetes with a body width of 6–8 mm, 1 mM AgNO<sub>3</sub> with polychaete crude extract of pH 9, preheated at 90°C for 15 min before incubation at 30°C (150 rpm) for 24 hours, and stored at 4°C for long-term stability. The formation of AgNPs was confirmed through observation of a color transition (from pinkish to yellowish-brown) and analysis of UV-Vis spectra (between 398 and 400 nm). Scanning electron microscopy and transmission electron microscopy revealed the formation of spherical AgNPs with an average size of approximately 40.19 nm. Further, the optimized AgNPs demonstrated high storage stability for up to 6 months without any agglomeration. It is believed that these parameters are eminently suitable for the production of stable biosynthesized AgNPs.

**Keywords:** Biosynthesis; *Marphysa moribidii*; Optimization; Polychaetes; Silver nanoparticles

### 1. Introduction

Research into nanotechnology has garnered significant interest worldwide over the last few decades due to its superior physical, chemical, and biological properties compared to its bulk form (Usman et al., 2018; Khalil et al., 2019). One of the most promising nanoparticles in the scientific world is silver nanoparticles (AgNPs).

\*Corresponding author's email: [waniryani@umt.edu.my](mailto:waniryani@umt.edu.my), Tel.: +609-6683176; Fax: +609-6683615  
doi: [10.14716/ijtech.v12i3.4303](https://doi.org/10.14716/ijtech.v12i3.4303)

These are 10 to 100 nm in size and have superior physicochemical and antimicrobial properties, mainly due to their large surface area per volume ratio (Jeevanandam et al., 2018). Accordingly, AgNPs have been incorporated in various fields, including diagnosis, therapeutics, electrical, antimicrobial action, and catalysis (Zhang et al., 2016; Lee and Jun, 2019; Nakamura et al., 2019).

Conventionally, AgNPs have been synthesized by utilizing physical and chemical methods, which are costly and produce substances that are harmful to organisms and the environment (Zhang et al., 2016). However, numerous chemical and physical methods have been substituted by biological approaches in the last few years (Nakamura et al., 2019) that are environmentally sustainable and economical, as no toxic or expensive chemicals are utilized in the synthesis (Lee and Jun, 2019). In biological synthesis, two main components are required to initiate synthesis: a silver precursor such as silver nitrate ( $\text{AgNO}_3$ ) and a biomolecule cocktail extracted from living organisms that concurrently act as reducing and stabilizing agents (Siddiqi et al., 2018). These biomolecules react with silver ion ( $\text{Ag}^+$ ) and are reduced to AgNPs of various forms and sizes and act as capping agents to stabilize AgNPs (Zhang et al., 2016).

Microorganisms and plants are commonly exploited as reducing agents in this method since they are widely available in nature (Lee and Jun, 2019; Nakamura et al., 2019). Synthesizing AgNPs from invertebrate marine sources (especially polychaetes) is a relatively recent process. The polychaete is commonly referred to as a segmented worm (or marine worm) and belongs to the class of Polychaeta (Phylum Annelida). Polychaetes are generally used as pollution indicators, fish broodstock, and fish bait (Gaete et al., 2017; Cole et al., 2018; Masimen et al., 2020). Previous studies have indicated that some marine polychaetes can synthesize AgNPs (Singh et al., 2014; Hussain et al., 2018). However, synthesis was initiated utilizing species other than *Marphysa moribidii* (locally known as 'ruat bakau'). This is from the *Eunicidae* family and is harvested locally to be used as bait worm for recreational or artisanal fisheries (Idris et al., 2014). Using *M. moribidii* as a reducing agent in AgNP synthesis can increase the polychaete's commercial value, especially in Malaysia.

Although *M. moribidii* extract can function as a reducing agent in AgNP synthesis, biological synthesis requires optimization to produce higher quality AgNPs with desirable traits for industrial purposes (Velgosova et al., 2017; Nair et al., 2018). Synthesis parameters such as the body width of polychaete, storage conditions of AgNPs, pH values, temperature, and precursor concentration can be manipulated to produce AgNPs of different shapes and sizes. Further, this optimization process can significantly stabilize AgNPs (Zhang et al., 2016). Thus, this paper presents the optimization process conditions for AgNP synthesis using *M. moribidii* by varying parameters such as the body width of polychaete, storage conditions of AgNPs,  $\text{AgNO}_3$  concentration, pH of polychaete crude extract, and the temperature during the pre-incubation period.

## 2. Methods

*Marphysa moribidii* samples were collected from sediments during low tide at a mangrove area in Malaysia. Polychaetes were then acclimatized in aquaria that mimicked the polychaete's natural habitat prior to the experiment.

### 2.1. General Procedure of AgNP Synthesis

Polychaete extraction was carried out as reported by Rosman et al. (2020). A total of 10 mL aqueous crude extract was mixed thoroughly with 90 mL of silver nitrate ( $\text{AgNO}_3$ ) (Bendosen, UK) and underwent dark incubation at 30°C (150 rpm) for 24 h. Two negative

control types were prepared by mixing 10 mL of double-distilled water (ddH<sub>2</sub>O) with 90 mL of 1 mM AgNO<sub>3</sub>. Commercial positive control AgNPs were purchased from Sigma Aldrich (USA). Samples were left at room temperature (30±2°C) after incubation and periodically checked for yellowish-brown color formation in the solution, which would indicate the formation of AgNPs (Ayad et al., 2019).

## 2.2. Effects of Different Body Width Classes of polychaete on AgNP Synthesis

Various polychaete classes were screened to analyze their potential for reducing Ag<sup>+</sup> to AgNPs. These polychaetes were categorized based on their body width: Class I (3–5 mm), Class II (6–8 mm), and Class III (9–11 mm). For each polychaete, the body widths of the first seven chaetigers were measured and expressed in mm (Górska et al., 2019). It should be noted that the width of chaetigers does not include parapodia or bristles.

### 2.2.1. Preparation of polychaete crude extract according to body width

Unwanted dirt particles from freshly killed polychaetes were removed by washing thoroughly using artificial seawater and then rinsed with ddH<sub>2</sub>O three times. A total of 10 g polychaetes of varying body widths were weighed, cut into fine pieces, homogenized using a WT-130 homogenizer (El Dorado Labtech), and mixed with 100 mL ddH<sub>2</sub>O solution (Rosman et al., 2020). The mixtures of three samples were incubated on the bench for 1 h before filtration with Whatman No. 1 filter paper (11 µm). Polychaete crude extraction was then performed on ice and stored at 4°C for further use.

## 2.3. Effects of Different Physical Parameters on AgNP Synthesis

The physical parameters were optimized using the polychaete crude extract with body widths obtained from the previous optimization. The color and absorbance of the resulting reaction mixture were measured spectrophotometrically. The optimal condition was determined according to the darkest yellowish-brown color of the solution with the highest UV-Vis absorbance reading (Ayad et al., 2018). All experiments were carried out in triplicate (n=3).

### 2.3.1. Effects of AgNO<sub>3</sub> concentration

A series of AgNO<sub>3</sub> concentrations (0.5, 1, 2, and 4 mM) was tested for the reaction mixture (Amini et al., 2017). Then, 10 mL of aqueous crude extract was mixed with 90 mL of AgNO<sub>3</sub> in various concentrations and subjected to dark incubation at 30°C (150 rpm) for 24 h.

### 2.3.2. Effects of crude extract pH

The pH of the crude extract was optimized at different pH values (3, 5, 7, 9, and 11) by adjusting the pH using 0.1 M HCl and 0.1 M NaOH according to the method described by Ndikau et al. (2017). Subsequently, 10 mL of aqueous crude extract in various pH values was then mixed with 90 mL of 1mM AgNO<sub>3</sub> and subjected to dark incubation at 30°C (150 rpm) for 24 h.

### 2.3.3. Effects of temperature during the pre-incubation period

Here, 10 mL of pH 9 aqueous crude extract was mixed with 90 mL of 1 mM AgNO<sub>3</sub>. The reaction mixture was then treated at various temperatures (4, 30, 50, 70, and 90 °C) throughout pre-incubation (30 min) without agitation before incubation at 30°C (150 rpm) for 24 h in the incubator shaker (Amini et al., 2017). The shapes of AgNPs synthesized at different temperatures during the pre-incubation period were analyzed using a transmission electron microscope (TEM).

### 2.3.4. Effects of different storage conditions on the stability of AgNPs

The reaction mixture was preserved under different conditions (room temperature of 30±2°C and in a fridge at 4°C) for seven days to research the stability of synthesized AgNPs

(Velgosova et al., 2017). The optimal storage condition was determined by changes in the surface plasmon resonance (SPR) peaks, which exhibited minimal shifts in absorbance and wavelengths.

#### 2.4. Characterization of Optimized AgNPs

Color changes of biosynthesized AgNPs were recorded through visual observations. The bio-reduction of AgNO<sub>3</sub> was confirmed from the SPR peak formation obtained by the UV-Visible spectrophotometer (UV-1800) (Shimadzu, Japan) at wavelengths ranging from 300 to 600 nm. The AgNP morphology was examined using scanning electron microscopy (SEM) (JSM-6390 LA (JEOL, USA)) at an accelerating voltage of between 15 and 20 kV. All samples were prepared by a mounting process. A drop of AgNPs was deposited onto dry poly-L-lysine and coated with gold via sputtering (Auto Fine Coater-JEOL) prior to analyses. The shape and average particle sizes of biosynthesized AgNPs were observed using TEM (Tecnai G2 Spirit Biotwin (USA)) at 120 kV. The samples were prepared by drop-casting diluted biosynthesized AgNPs on a coated copper grid. The residual solution was then dried using blotting paper, and TEM measurements were performed at ambient temperature. Image J software was used to predict the average size of the AgNPs.

### 3. Results and Discussion

Optimization was carried out to enhance the stability, yield, and characteristics of the AgNPs. UV-Vis spectra analysis of all optimizations was conducted at Week 4, indicating a maximum reduction of AgNO<sub>3</sub> to AgNPs except for optimizing storage conditions, which were only observed at Day 7. In this research, the biomolecules of the polychaete crude extract served as both reducing and stabilizing agents for AgNP synthesis. The first evidence of the presence of AgNPs was the gradual color changes of a pinkish solution to yellowish-brown due to the excitation of surface plasmon vibrations when the polychaete extracts were mixed with AgNO<sub>3</sub> precursor (Ayad et al., 2019). Surface plasmon resonance (SPR) occurs when conduction electrons in AgNPs undergo a collective oscillation when induced by light at specific wavelengths, which has become a vital characterization in nanoparticle synthesis (Zhang et al., 2016). Further confirmation of the existence of AgNPs was the formation of UV-Vis absorption peaks between 380 and 450 nm (due to the SPR phenomenon) and the reduction of AgNO<sub>3</sub> (Ndikau et al., 2017). According to the literature, the absorption band in the range of 380–450 nm in the UV-Vis spectra might be attributable to the AgNPs (Chowdhury et al., 2016; Vinayagam et al., 2018). Moreover, it is well established that SPR bands are susceptible to and highly dependent on the size and shape of the nanoparticles, the AgNO<sub>3</sub> concentration, and the type of biomolecules presented in the biological extract (Raja et al., 2017; Ruttkay-nedecky et al., 2019). Figure 1 illustrates the mechanism of AgNP formation and the differences between solution colors of polychaete crude extract, AgNO<sub>3</sub> solution, and biosynthesized AgNPs.

#### 3.1. Optimization of Polychaete Classes according to Body Widths

A range of polychaete age classes were used to research their effects on AgNP synthesis. Body width is a standard technique for determining the polychaete age class (Occhioni et al., 2010). Hence, *M. moribidii* was categorized into three main classes according to body width: Class I (3–5 mm, young), Class II (6–8 mm, adult), and Class III (9–11 mm, old). Exposure of AgNO<sub>3</sub> to crude extracts of various age classes of polychaetes was shown to affect the biosynthesis of AgNPs, as depicted in Figure 2. Further, Figure 2a reveals that only the solution of AgNPs synthesized from Class II polychaetes turned yellowish-brown, indicating the formation of AgNPs.

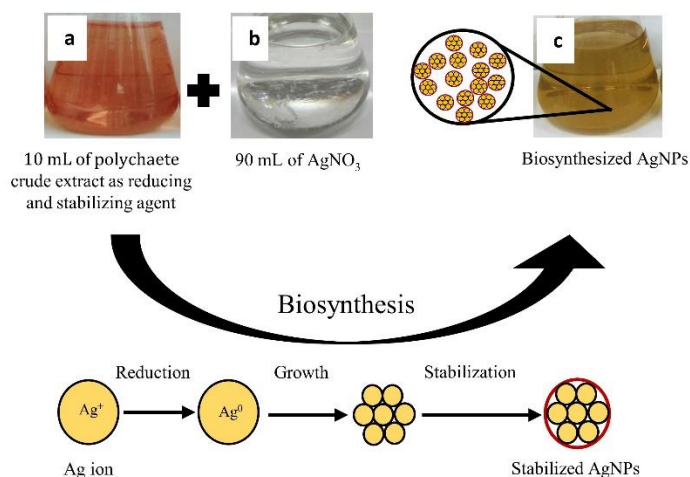


**Figure 1** Mechanism of AgNP synthesis utilizing a crude polychaete extract (*M. moribidii*): (a) Polychaete crude extract; (b) Precursor  $\text{AgNO}_3$ ; and (c) Biosynthesized AgNPs

By comparison, the solutions of AgNPs synthesized from Class I and III polychaetes were found to be cloudy and light greenish-yellow, indicating no AgNP formation. Further analysis was possible by observing changes in the SPR bands of AgNPs synthesized using Class I, Class II, and Class III polychaetes. The SPR band of biosynthesized AgNPs from Class II polychaete exhibited a broad peak at 396.50 nm, confirming the formation of AgNPs (as presented in Figure 2b). This broad absorption peak implied larger biosynthesized AgNPs (Ndikau et al., 2017). Moreover, no visible peak was detected from the SPR band from both reaction mixtures containing Class I and Class III polychaetes, confirming no AgNP formation. The negative control of  $\text{AgNO}_3$  and the positive control of AgNPs from Sigma Aldrich exhibited a persistent SPR band throughout the experimental period.

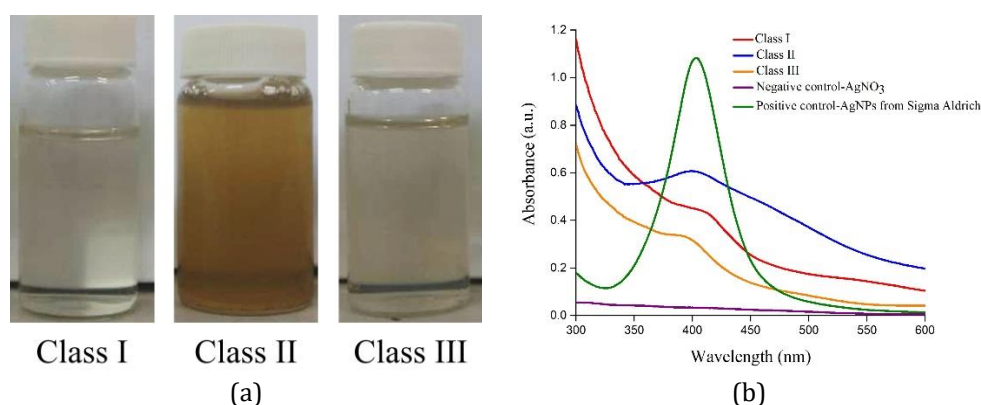


**Figure 2** AgNPs synthesized from various body widths of *M. moribidii* (Class I, Class II, and Class III): (a) Color changes at Week 4; and (b) Analysis of UV-Vis spectra

The occurrence of biosynthesized AgNPs was suggested as being attributable to the reduction of silver ion ( $\text{Ag}^+$ ) to AgNPs ( $\text{Ag}^0$ ), mediated by electron shuttle from the oxidation of reducing agents (El-Seedi et al., 2019). Further, research suggested that different ages of samples might produce a different nature of the biogenic reducing agent. The older polychaetes (Class III) produced AgNPs with undesirable characteristics, and the less stable condition might be due to the weak activity of the bioactive compound, which is supposed to act as a reducing agent and/or stabilizer. Similarly, AgNPs produced from young *Fusarium oxysporum* achieved superior results compared to the older cultures with a

similar incubation time (Shahzad et al., 2019). However, AgNPs synthesized from Class II polychaetes exhibited a superior result compared to Class I polychaetes. A possible reason for this is the augmented level of reducing agents in the Class II polychaetes responsible for  $\text{Ag}^+$  reduction. As Class I polychaetes were young, the concentrations of reducing and stabilizing agents might have been inadequate.

It has been proposed that sterols, proteins, phenols, fatty acids, ether, and carbohydrates in the polychaete crude extract can probably synthesize and stabilize AgNPs (Singh et al., 2014; Pei et al., 2020; Rosman et al., 2020). These functional groups could have reacted with  $\text{Ag}^+$  to produce AgNPs and subsequently prevent agglomeration of AgNPs, as reported in other studies (Pei et al., 2020; Rosman et al., 2020).

### 3.2. Effects of Different Physical Parameters on AgNPs Synthesis

#### 3.2.1. Optimization of $\text{AgNO}_3$ concentration

Based on Figure 3a, yellowish-brown colors were observed in AgNP solutions synthesized utilizing 0.5 and 1 mM of  $\text{AgNO}_3$  concentrations. However, beyond these concentrations (2 and 4 mM of  $\text{AgNO}_3$ ) the solutions turned cloudy and light greenish-yellow, indicating no formation of AgNPs. According to the UV-Vis spectra (Figure 3b), the absorbance of the SPR peak of AgNPs increased slightly from 0.5 mM (1.34) to 1 mM (1.54) and then plateaued from 2 to 4 mM of  $\text{AgNO}_3$ . Further, AgNPs synthesized from 2 mM onwards were not stable during the experiment, and the aggregation of newly formed AgNPs could be observed. The SPR peaks of AgNPs synthesized using 0.5 and 1 mM  $\text{AgNO}_3$  were 393 and 399 nm, respectively, validating the formation of AgNPs. However, both SPR peaks of AgNPs synthesized using 0.5 and 1 mM  $\text{AgNO}_3$  still exhibited a wide peak, indicating that the particles were polydispersed (Ashraf et al., 2016).

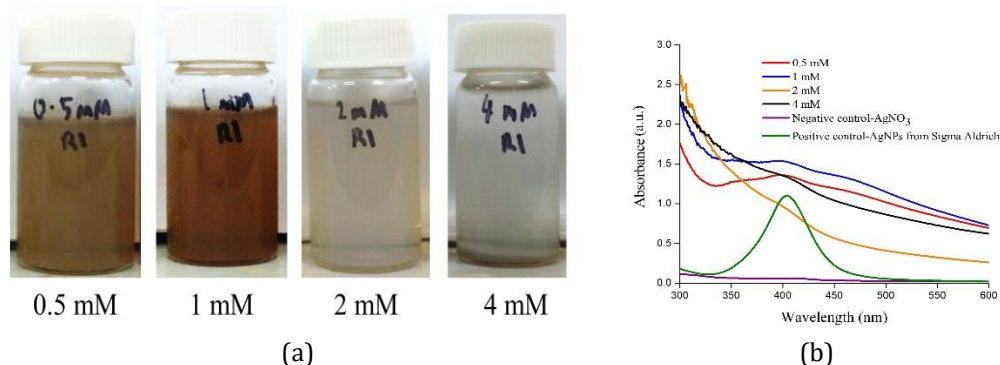


**Figure 3** AgNPs synthesized using Class II polychaete and  $\text{AgNO}_3$  of different concentrations (0.5, 1, 2, and 4 mM) of  $\text{AgNO}_3$ : (a) Color changes at Week 4; and (b) Analysis of UV-Vis spectra

These results provided some evidence that varying concentrations of  $\text{AgNO}_3$  up to 1 mM resulted in a complete reduction of  $\text{Ag}^+$ . Precipitates formed beyond this concentration might be explained according to the theory of redox reaction. It is possible that the number of electrons carried by a reducing agent is not sufficient to facilitate the reduction of excess  $\text{Ag}^+$  in the concentrated solution. Hence,  $\text{AgNO}_3$  was not completely reduced by the crude extract. This resulted in the generation of larger sizes of AgNPs due to AgNP aggregation with unreacted  $\text{AgNO}_3$  (Bhatnagar et al., 2019). These results are in agreement with other studies in which the possibility of particle agglomeration increased at higher concentrations (Raman et al., 2015; Shahzad et al., 2019).

### 3.2.2. Optimization of crude extract pH

According to Figure 4a, the AgNPs synthesized using the crude extract of Class II polychaete and 1 mM AgNO<sub>3</sub> with different pH values produced different colors. The crude extract color instantly changed from pinkish to brownish when the pH value was adjusted to 3 and 5. The crude extracts maintained their original pinkish color when the pH value was increased to 7, 9, and 11. After synthesis, the color of the AgNP solution at higher pH values (7, 9, and 11) gradually changed to yellowish-brown, indicating the formation of AgNPs (as shown in Figure 4b). An AgNP solution synthesized at pH 9 exhibited a darker brown color, suggesting higher levels of AgNPs at pH values of 7, 9, 11. These results were confirmed by analyzing the UV-Vis spectra, in which the maximum absorbance of AgNPs was at pH 9 (0.72), followed by pH 7 (0.64), pH 5 (0.58), and pH 11 (0.53), as presented in Figure 4c. Furthermore, an increment in pH values from 5 to 9 narrowed the SPR peak, suggesting that the size of AgNPs reduced with an increase in pH (Karekalammanavar and David, 2018). No peak was detected from a reaction mixture containing pH 3 crude extract. Moreover, the SPR peaks of AgNP solutions synthesized from polychaete crude extract with pH values of 5–11 appeared between 390.00 and 396.50 nm.

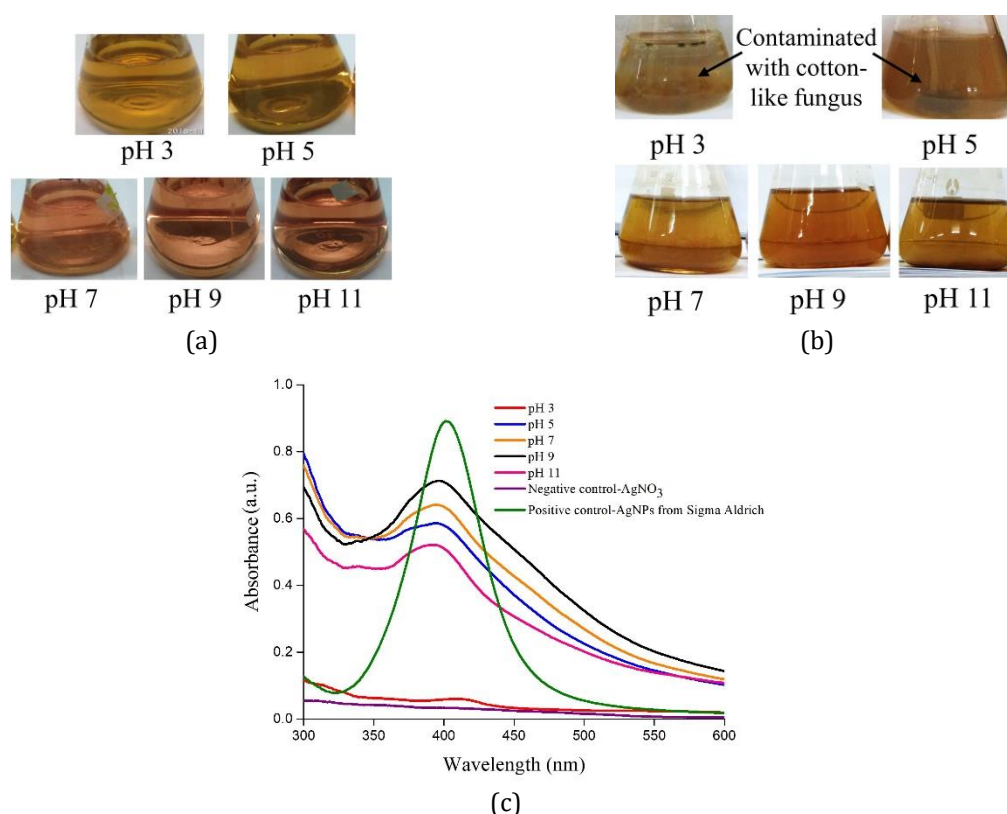


**Figure 4** AgNPs synthesized using 1 mM AgNO<sub>3</sub> and polychaete crude extract Class II with different pH values (3, 5, 7, 9, and 11): (a) Color of polychaete crude extract Class II adjusted to different pH values (3, 5, 7, 9, and 11) before the addition of AgNO<sub>3</sub>; (b) Color changes at Week 4; and (c) Analysis of UV-Vis spectra. AgNP solutions synthesized from crude extract with pH 3 and pH 5 were visibly contaminated with cotton-like fungus (indicated by arrows).

Higher pH values facilitated a complete reduction of Ag<sup>+</sup> to AgNPs by providing electrons, eventually forming many AgNPs with smaller diameters (Saxena et al., 2016). The aggregation of AgNPs tends to dominate the nucleation process in acidic conditions. At lower pH values (acidic), a large quantity of H<sup>+</sup> is available to neutralize the negatively charged functional group of the reducing agent (Ndikau et al., 2017). Thus, the activity of a

reducing agent is reduced. At higher pH values (alkaline), a large amount of  $\cdot\text{OH}$  is available in the solution, which will attract  $\text{H}^+$  from a reducing agent, leaving a negatively charged functional group (Ndikau et al., 2017). Thus, many functional groups are available for binding to  $\text{AgNO}_3$ , facilitating a higher number of  $\text{Ag}^+$  to bind and form AgNPs with smaller diameters.

If the number of AgNPs increases substantially, there is a possibility that degradation and agglomeration may occur in the solution, decreasing the stability of synthesized AgNPs (Ahmad et al., 2013). This phenomenon was observed when synthesizing AgNPs at pH 11, which exhibited the lowest SPR absorbance. As the reducing agent's reduction ability was intact until pH 9, the aggregation could have occurred due to a lack of stabilizing agents with respect to the number of excess AgNPs produced. Similar findings were documented on *Hippophae rhamnoides* (sea buckthorn) aqueous leaf extract (Ahmad et al., 2013) and *Citrus sinensis* (sweet orange) peel extract (Nair et al., 2018) mediated AgNP synthesis.

### 3.2.3. Optimization of temperature during the pre-incubation period

In this section, the influence of temperature (4, 30, 50, 70, and 90 °C) during the pre-incubation period was analyzed in AgNP synthesis. Here, the AgNPs were synthesized using 1 mM of  $\text{AgNO}_3$  and pH 9 polychaete crude Class II. Figure 5a shows the color variations during pre-incubation (30 min). The reaction mixture solution treated at 90 and 70 °C changed color after 15 and 30 min, respectively. No color changes were observed by the reaction mixture treated at 4, 30, and 50 °C. Generally, the AgNP solution color gradually turned darker in conjunction with increasing observation times. As shown in Figure 5b, the AgNP solution's color became darker as the temperature increased from 70 to 90 °C during the pre-incubation period.

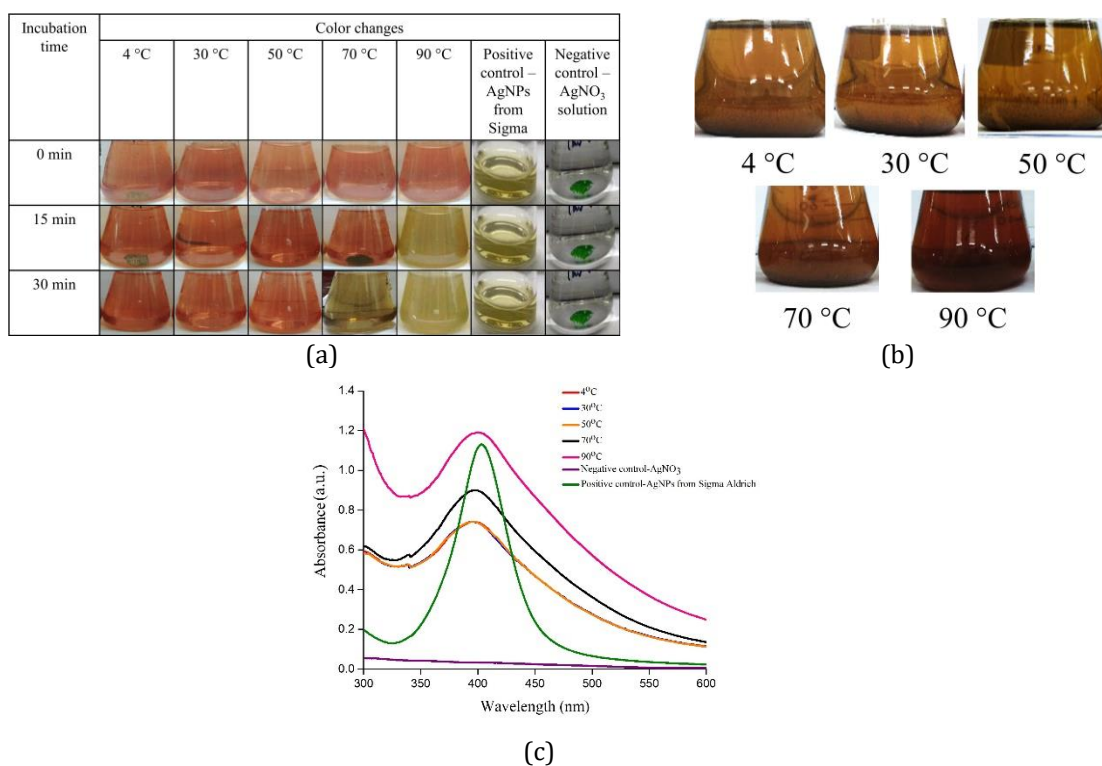


**Figure 5** AgNPs synthesized using 1 mM of  $\text{AgNO}_3$  and pH 9 polychaetes crude Class II at different temperatures (4, 30, 50, 70, and 90 °C) during the pre-incubation period: (a) Color changes indicate the reduction of  $\text{Ag}^+$  activity to AgNPs by *M. moribidii* extract occurred during pre-incubation (30 min); (b) Color changes at Week 4; and (c) Analysis of UV-Vis spectra

Moreover, according to the UV-Vis spectra results (Figure 5c), the SPR absorbance of AgNPs synthesized at 4, 30, and 50°C during the pre-incubation period was found to be similar (approximately 0.77). Nevertheless, an increase in temperature above 70°C increased the absorbance reading (0.90), indicating an improvement in the concentration of AgNPs. The highest SPR absorbance of AgNPs was observed at 90°C (1.19), suggesting maximum AgNP synthesis. This was because high temperatures impart increased kinetic energy, resulting in faster synthesis rates (Verma and Mehata et al., 2016). The SPR peaks of synthesized AgNPs treated at different temperatures during the pre-incubation period presented the range 396.00–399.50 nm.

It is also suggested that temperature is a crucial factor for manipulating the shape of synthesized AgNPs (Lee et al., 2014). Based on TEM images (Figure 6), various shapes of AgNPs were generated when treated at 4°C (rectangular and spherical), 30°C (hexagonal, rectangular, and spherical), 50°C (rectangular, triangular, and spherical), and 70°C (triangular and spherical) during the pre-incubation period. Uniformly spherical AgNPs were synthesized at 90°C, which can be described by the concept of thermodynamics. Lee et al. (2014) reported that silver atoms cannot rearrange their occupied positions easily during the nucleation process due to insufficient kinetic energy. However, the kinetic energy of the molecules increases and Ag<sup>+</sup> is consumed more rapidly at higher temperatures (90°C), leaving less possibility for particle size growth (Jain and Mehata, 2017). Thus, spherical particles of nearly uniform size distribution are formed at higher temperatures.

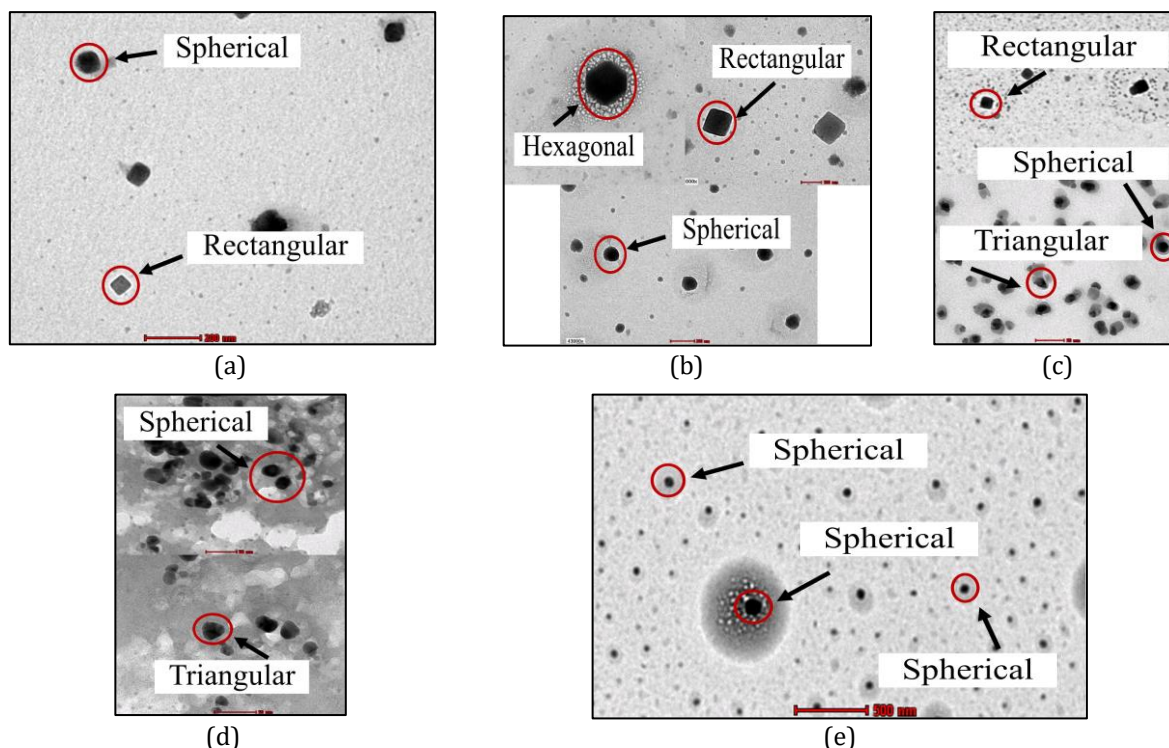


**Figure 6** Various shapes of AgNPs biosynthesized at different temperatures during the pre-incubation period observed using TEM: (a) 4°C; (b) 30°C; (c) 50°C; (d) 70°C; and (e) 90°C. All AgNPs synthesized at 90 °C during the pre-incubation period were spherical

#### 3.2.4. Optimization of storage condition of synthesized

After synthesis, the AgNP solutions were maintained at room temperature and 4°C. Shifts in the UV-Vis wavelength and changes in AgNP solutions were monitored daily for

one week. The results revealed that AgNP solutions stored at room temperature (Figure 7a) exhibited a visible shift in the SPR band from 413 to 403 nm compared to the AgNP solution stored at 4°C, which remained at 413 nm throughout the experiment (Figure 7b). The SPR absorbance of AgNPs stored at room temperature significantly decreased from 0.73 to 0.49 in just seven days. This decrease in absorption intensity with a broad SPR band indicated the aggregation and broad particle size distribution of AgNPs (Mishra et al., 2013). In contrast, the SPR absorbance of AgNPs stored at 4°C slightly decreased from 0.73 to 0.67, and the peak was still intact at day seven. These results indicated that a temperature of 4°C slowed down the AgNP destabilization process compared to room temperature.

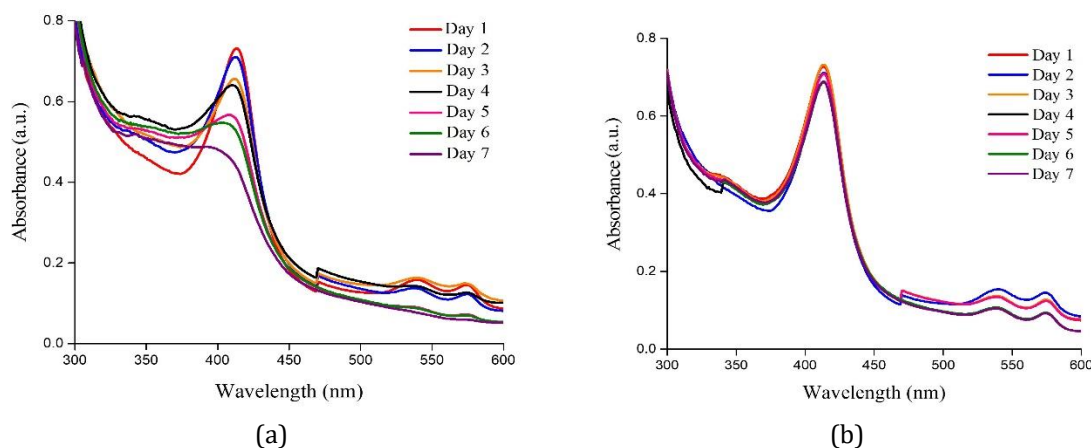


**Figure 7** UV-Vis spectra of biosynthesized AgNPs solutions stored at different temperature from day 1 to day 7: (a) Room temperature (30°C±2); and (b) 4°C

Any loss of AgNP stability can reduce the effectiveness of AgNPs' properties. Further, AgNPs are likely to modify their properties over time and can even synthesize under optimized conditions (Muñoz et al., 2019). The stability of AgNPs depends on both the optimization of AgNP synthesis and storage conditions to maintain the functionality of the capping agent used for stabilization. Many factors can influence AgNP destabilization, such as higher storage temperatures, exposure to sunlight, type of biomolecules presented in the biological extract, nature of the capping agent, and the stabilization mechanism (Izak-Nau et al., 2015). In addition, the stability of AgNPs was reported as mainly dependent on electrical charges on the surface of AgNPs, which were stable at low temperatures (Velgosova et al., 2017). Therefore, maintaining the charge of AgNPs in the solution seems to be crucial for maintaining the stability and biological effects.

### 3.3. Characterization of optimized AgNPs

Figure 8 shows the characterization of optimized AgNPs synthesized from *M. moribidii*. The conditions were as follows: 1 mM concentration of AgNO<sub>3</sub> with polychaete crude extract pH 9, treated at 90°C during the pre-incubation period for 15 min before incubation at 30°C (150 rpm) for 24 hours, and stored at 4°C for long-term storage. The color of optimized AgNPs was retained without any agglomeration through observations for six months, as shown in Figure 8a. Further, the SPR peak of optimized AgNPs was maintained at 398–400 nm, as displayed in Figure 8b. The biosynthesized AgNPs were further categorized by SEM and TEM. The SEM analysis confirmed the formation of spherical-shaped AgNPs in higher densities and confirmed the development of AgNPs, as presented in Figure 8c. By comparison, TEM analysis revealed spherical AgNPs with an average size of 40.19 nm, as shown in Figure 8d. The larger particles may have resulted from particle aggregation.

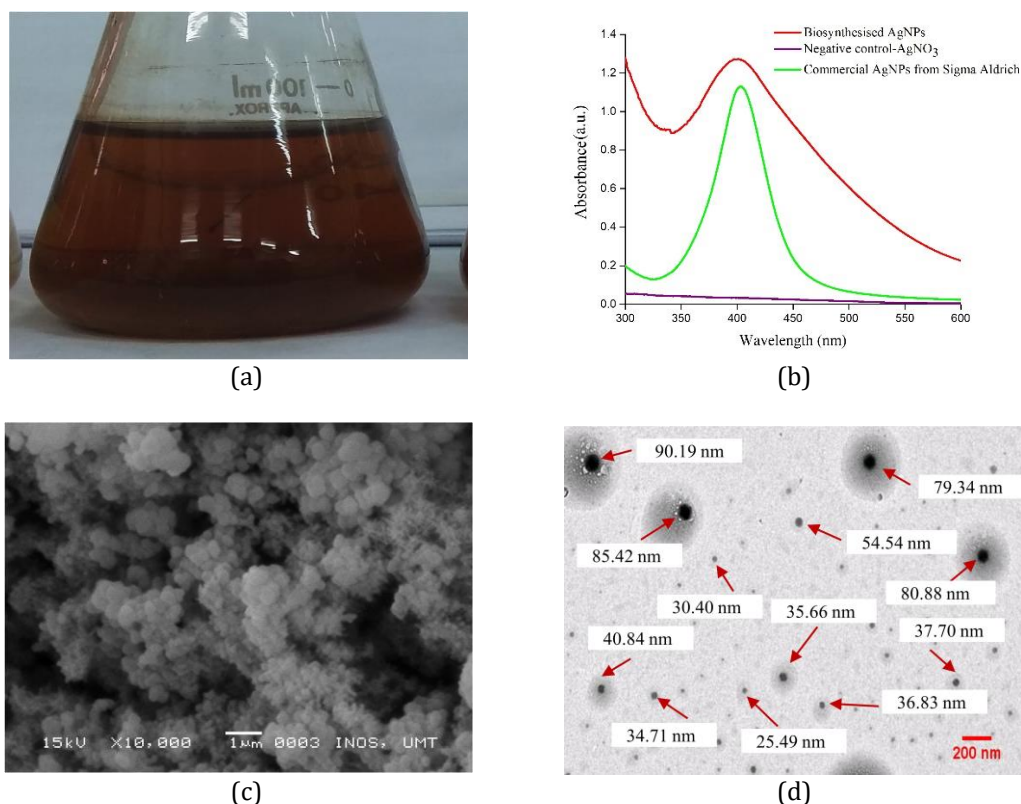


**Figure 8** Characterization of optimized AgNPs after six months: (a) Color of optimized AgNPs maintained at 4°C; (b) UV-Vis spectra of optimized AgNPs; (c) SEM result; and (d) TEM result

#### 4. Conclusions

This research has demonstrated the successful optimization of biogenic AgNPs synthesized from marine polychaete (*M. moribidii*). The protocol was optimized, offering rapid production of AgNPs with increased stability and characteristics. The present investigation concluded that the green synthesis of AgNPs utilizing marine invertebrates (*M. moribidii*) as reducing and stabilizing agents offered many advantages. These included being economical, straightforward, and eco-friendly, which can scale up economic viability. Future studies could consider exploring possible applications of biosynthesized AgNPs, especially in healthcare. The findings of this research can be useful as a reference for biogenic AgNPs and green nanotechnology research, with the aim of discovering more marine polychaetes with the potential to be utilized as reducing and stabilizing agents in AgNP synthesis.

#### Acknowledgements

We would like to thank the Ministry of Higher Education, Malaysia, and the Universiti Malaysia Terengganu for their funding (FRGS/1/2016/WAB09/UMT/02/2).

#### References

- Ahmad, B., Ali, J., Bashir, S., 2013. Optimization and Effects of Different Reaction Conditions for the Bioinspired Synthesis of Silver Nanoparticles using *Hippophae rhamnoides* Linn. Leaves Aqueous Extract. *World Applied Sciences Journal*, Volume 22(6), pp. 836–843
- Amini, N., Amin, G., Azar, Z.J., 2017. Green Synthesis of Silver Nanoparticles using *Avena sativa* Leaves Extract. *Nanomedicine Research Journal*, Volume 2(1), pp. 57–63

- Ashraf, J.M., Ansari, M.A., Khan, H.M., Alzohairy, M.A., Choi, I., 2016. Green Synthesis of Silver Nanoparticles and Characterization of their Inhibitory Effects on AGEs Formation using Biophysical Techniques. *Scientific Reports*, Volume 6(20414), pp. 1–10
- Ayad, Z.M., Ibrahim, O.M.S., Omar, L.W., 2019. Biosynthesis and Characterization of Silver Nanoparticles by *Silybum marianum* (silymarin) Fruit Extract. *Advances in Animal and Veterinary Sciences*, Volume 7(2), pp. 122–130
- Bhatnagar, S., Kobori, T., Ganesh, D., Ogawa, K., Aoyagi, H., 2019. Biosynthesis of Silver Nanoparticles Mediated by Extracellular Pigment from *Talaromyces purpurogenus* and their Biomedical Applications. *Nanomaterials*, Volume 9(7), pp. 1–20
- Chowdhury, S., Yusof, F., Faruck, M.O., Sulaiman, N., 2016. Process Optimization of Silver Nanoparticle Synthesis using Response Surface Methodology. *Procedia Engineering*, Volume 148, pp. 992–999
- Cole, V.J., Chick, R.C., Hutchings, P.A., 2018. A Review of Global Fisheries for Polychaete Worms as a Resource for Recreational Fishers: Diversity, Sustainability and Research Needs. *Reviews in Fish Biology and Fisheries*, Volume 28, pp. 543–565
- El-Seedi, H.R., El-Shabasy, R.M., Khalifa, S.A.M., Saeed, A., Shah, A., Shah, R., Iftikhar, F.J., Abdel-Daim, M.M., Omri, A., Hajrahand, N.H., Sabir, J.S.M., Zou, X., Halabi, M.F., Sarhan, W., Guo, W., 2019. Metal Nanoparticles Fabricated by Green Chemistry using Natural Extracts: Biosynthesis, Mechanisms, and Applications. *RSC Advances*, Volume 9(42), pp. 24539–24559
- Gaete, H., Álvarez, M., Lobos, G., Soto, E., Jara-Gutiérrez, C., 2017. Assessment of Oxidative Stress and Bioaccumulation of the Metals Cu, Fe, Zn, Pb, Cd in the Polychaete *Perinereis gualpensis* from Estuaries of Central Chile. *Ecotoxicology and Environmental Safety*, Volume 145, pp. 653–658
- Górska, B., Gromisz, S., Włodarska-Kowalczyk, M., 2019. Size Assessment in Polychaete Worms—Application of Morphometric Correlations for Common North Atlantic Taxa. *Limnology and Oceanography: Methods*, Volume 17(4), pp. 254–265
- Hussain, N.S., Harun, N.A., Radzi, M.N.F., Idris, I., Wan Ismail, W.I., 2018. Biosynthesis of Silver Nanoparticles from Marine Polychaete *Diopatra claparedii* Grube, 1878. *Jurnal Teknologi*, Volume 80(6), pp. 181–187
- Idris, I., Hutchings, P., Arshad, A., 2014. Description of a New Species of *Marphysa* Quatrefages, 1865 (Polychaeta: Eunicidae) from the West Coast of Peninsular Malaysia and Comparisons with Species from *Marphysa* Group A from the Indo-West Pacific and Indian Ocean. *Memoirs of Museum Victoria*, Volume 71, pp. 109–121
- Izak-Nau, E., Huk, A., Reidy, B., Uggerud, H., Vadset, M., Eiden, S., Voetz, M., Himly, M., Duschl, A., Dusinska, M., Lynch, I., 2015. Impact of Storage Conditions and Storage Time on Silver Nanoparticles' Physicochemical Properties and Implications for their Biological Effects. *RSC Advances*, Volume 5(102), pp. 84172–84185
- Jain, S., Mehata, M.S., 2017. Medicinal Plant Leaf Extract and Pure Flavonoid Mediated Green Synthesis of Silver Nanoparticles and their Enhanced Antibacterial Property. *Scientific Reports*, Volume 7(1), p. 1–13
- Jeevanandam, J., Barhoum, A., Chan, Y.S., Dufresne, A., Danquah, M.K., 2018. Review on Nanoparticles and Nanostructured Materials: History, Sources, Toxicity and Regulations. *Beilstein Journal of Nanotechnology*, Volume 9(1), pp. 1050–1074
- Karekalammanavar, G., David, M., 2018. Optimization of Green Synthesis of Silver Nanoparticles from Leaf Extracts of *Tabernaemontana heyneana* and Evaluation of their Catalytic Activity on Reduction of Methylene Blue. *Haya: The Saudi Journal of Life Sciences*, Volume 3(3), pp. 248–254

- Khalil, M., Rahmaningsih, G., Gunlazuardi, J., Umar, A., 2019. The Influence of Plasmonic Au Nanoparticle Integration on the Optical Bandgap of Anatase TiO<sub>2</sub> Nanoparticles. *International Journal of Technology*, Volume 10(4), pp. 808–817
- Lee, S., Jun, B.H., 2019. Silver Nanoparticles: Synthesis and Application for Nanomedicine. *International Journal of Molecular Sciences*, Volume 20(4), pp. 865–885
- Lee, S.W., Chang, S.H., Lai, Y.S., Lin, C.C., Tsai, C.M., Lee, Y.C., Chen, J.C., Huang, C.L., 2014. Effect of Temperature on the Growth of Silver Nanoparticles using Plasmon-Mediated Method under the Irradiation of Green LEDs. *Journal of Material*, Volume 7(12), pp. 7781–7798
- Masimen, M.A.A., Harun, N.A., Misbah, S., Idris, I., Wan Ismail, W.I., 2020. Marine Resources: Potential of Polychaete Application in Combating COVID-19 Infection. *Journal of Sustainability Science and Management*, Volume 15(7), pp. 1–7
- Mishra, A., Kaushik, N.K., Sardar, M., Sahal, D., 2013. Evaluation of Antiplasmodial Activity of Green Synthesized Silver Nanoparticles. *Colloids and Surfaces B: Biointerfaces*, Volume 111, pp. 713–718
- Muñoz, R.V., Jimenez, M.J.A, Lopez, F.D., Ribot, J.L.L., 2019. Protocol Optimization for a Fast, Simple and Economical Chemical Reduction Synthesis of Antimicrobial Silver Nanoparticles in Non-specialized Facilities. *BMC Research Notes*, Volume 12(1), pp. 773–779
- Nair, S.S., Rizvi, S.T., Anthappan, P.D., 2018. Optimization of Rapid Green Synthesis of AgNPs using *Citrus Sinensis* Peel Extract for Antibacterial Activity. *International Journal of Advanced Scientific Research and Management*, Volume 3(8), pp. 274–281
- Nakamura, S., Sato, M., Sato, Y., Ando, N., Takayama, T., Fujita, M., Ishihara, M., 2019. Synthesis and Application of Silver Nanoparticles (AgNPs) for the Prevention of Infection in Healthcare Workers. *International Journal of Molecular Sciences*, Volume 20(15), pp. 3620–3638
- Ndikau, M., Noah, N.M., Andala, D.M., Masika, E., 2017. Green Synthesis and Characterization of Silver Nanoparticles using *Citrullus lanatus* Fruit Rind Extract. *International Journal of Analytical Chemistry*, Volume 2017, pp. 1–9
- Occhioni, G.E., Brasil, A.C.S., Araújo, A.F.B., 2010. Morphometric study of *Phragmatopoma caudata* (Polychaeta: Sabellida: Sabellariidae). *Zoologia (Curitiba)*, Volume 26(4), pp. 739–746
- Pei, A.U.E., Huai, P.C., Masimen, M.A.A., Wan Ismail, W.I., Idris, I., Harun, N. A., 2020. Biosynthesis of Gold Nanoparticles (AuNPs) by Marine Baitworm *Marphysa moribidii* Idris, Hutchings and Arshad 2014 (Annelida: Polychaeta) and its Antibacterial Activity. *Advances in Natural Sciences: Nanoscience and Nanotechnology*, Volume 11(1), pp. 1–10
- Raja, S., Ramesh, V., Thivaharan, V., 2017. Green Biosynthesis of Silver Nanoparticles using *Calliandra haematocephala* Leaf Extract, their Antibacterial Activity and Hydrogen Peroxide Sensing Capability. *Arabian Journal of Chemistry*, Volume 10(2), pp. 253–261
- Raman, P.R., Parthiban, S., Srinithya, B., Kumar, V.V., Anthony, S.P., Sivasubramanian, A., Muthuraman, M.S., 2015. Biogenic silver Nanoparticles Synthesis using the Extract of The Medicinal Plant *Clerodendron serratum* and Its *In-Vitro* Antiproliferative Activity. *Materials Letters*, Volume 160, pp. 400–403
- Rosman, N.S.R., Harun, N.A., Idris, I., Wan Ismail, W.I., 2020. Eco-friendly Silver Nanoparticles (AgNPs) Fabricated by Green Synthesis using the Crude Extract of Marine Polychaete, *Marphysa moribidii*: Biosynthesis, Characterization, and Antibacterial Applications. *Heliyon*, Volume 6(11), pp. 1–9

- Ruttikay-nedecky, B., Skalickova, S., Kepinska, M., Cihalova, K., Docekalova, M., Stankova, M., Uhlirova, D., Fernandez, C., Sochor, J., Milnerowicz, H., Beklova, M., Kizek, R., 2019. Development of New Silver Nanoparticles Suitable for Materials with Antimicrobial Properties. *Journal of Nanoscience and Nanotechnology*, Volume 19(5), pp. 2762–2769
- Saxena, J., Sharma, P.K., Sharma, M.M., Singh, A., 2016. Process Optimization for Green Synthesis of Silver Nanoparticles by *Sclerotinia sclerotiorum* MTCC 8785 and Evaluation of Its Antibacterial Properties. *SpringerPlus*, Volume 5(1), pp. 1–10
- Shahzad, A., Saeed, H., Iqtedar, M., Hussain, S.Z., Kaleem, A., Abdullah, R., Sharif, S., Naz, S., Saleem, F., Aihetasham, A., Chaudhary, A., 2019. Size-Controlled Production of Silver Nanoparticles by *Aspergillus fumigatus* BTCC10: Likely Antibacterial and Cytotoxic Effects. *Journal of Nanomaterials*, Volume 2019, pp. 1–14
- Siddiqi, K. S., Husen, A., Rao, R. A. K., 2018. A Review on Biosynthesis of Silver Nanoparticles and their Biocidal Properties. *Journal of Nanobiotechnology*, Volume 16(1), pp. 14–42
- Singh, R., Sahu, S.K., Thangaraj, M., 2014. Biosynthesis of Silver Nanoparticles by Marine Invertebrate (Polychaete) and Assessment of Its Efficacy against Human Pathogens. *Journal of Nanoparticles*, Volume 2014, pp. 1–7
- Usman, A., Kusriani, E., Widiatoro, A.B., Hardiya, E., Abdullah, N.A., Yulizar, Y., 2018. Fabrication of Chitosan Nanoparticles Containing Samarium Ion Potentially Applicable for Fluorescence Detection and Energy Transfer. *International Journal of Technology*, Volume 9(6), pp. 1112–1120
- Vinayagam, R., Varadavenkatesan, T., Selvaraj, R., 2018. Green Synthesis, Structural Characterization, and Catalytic Activity of Silver Nanoparticles Stabilized with *Bridelia retusa* Leaf Extract. *Green Processing and Synthesis*, Volume 7(1), pp. 30–37
- Velgosova, O., Čižmarová, E., Málek, J., Kavuličova, J., 2017. Effect of Storage Conditions on Long-term Stability of Ag Nanoparticles Formed Via Green Synthesis. *International Journal of Minerals, Metallurgy, and Materials*, Volume 24(10), pp. 1177–1182
- Verma, A., Mehata, M.S., 2016. Controllable Synthesis of Silver Nanoparticles using Neem Leaves and their Antimicrobial Activity. *Journal of Radiation Research and Applied Sciences*, Volume 9(1), pp. 109–115
- Zhang, X.F., Liu, Z.G., Shen, W., Gurunathan, S., 2016. Silver Nanoparticles: Synthesis, Characterization, Properties, Applications, and Therapeutic Approaches. *International Journal of Molecular Sciences*, Volume 17(9), p. 1534